Effects of Mg accumulation on chemical and electronic properties of Mg-doped *p*-type GaN surface

Tamotsu Hashizume[a)]
Research Center for Integrated Quantum Electronics (RCIQE), Hokkaido University, Sapporo 060-8628, Japan

(Received 3 December 2002; accepted 16 April 2003)

Chemical and electronic properties of Mg-doped *p*-GaN surfaces were systematically investigated by x-ray photoelectron spectroscopy (XPS) and Auger electron spectroscopy (AES). The doping density of Mg ranged from 3×10^{19} to $9\times10^{19}\,\mathrm{cm}^{-3}$. The XPS and AES analyses revealed the accumulation of Mg for all the air-exposed and chemically treated *p*-GaN surfaces. The apparent density of Mg calculated from the XPS integrated intensity and the AES intensity was more than one order higher than the value in bulk determined by secondary ion mass spectroscopy. Mg accumulation as well as large amounts of oxides made up the disordered region on the *p*-GaN:Mg surfaces. Large surface band bending of 1.2–1.6 eV was found at the *p*-GaN surfaces even after treatment in KOH and NH_4OH solutions, due to the existence of high-density surface states. It was found that electron cyclotron resonance assisted N_2 -plasma treatment at 300 °C for 1 min is very effective in removing such surface disordered regions and reducing surface band bending. © *2003 American Institute of Physics.* [DOI: 10.1063/1.1580195]

I. INTRODUCTION

Acceptor doping with Mg is the most common method for achieving *p*-type conducting GaN. However, the large acceptor ionization energy of 200–300 meV leads to a high concentration of unionized Mg atoms in the range of $10^{19}\,\mathrm{cm}^{-3}$ or higher in GaN at room temperature (RT). Reboredo and Pantelides[1] predicted from theoretical calculation that defect complexes that involve interstitial Mg account for the high degree of Mg incorporation into electrically inactive form. Several groups reported[2–5] that different kinds of defects, namely, pyramidal defects accompanied by Mg accumulation or segregation, formed in GaN:Mg and affected the optical and electrical properties of Mg-doped *p*-type GaN. Furthermore, the ''memory'' and ''surface segregation'' effects of Mg during epitaxial growth[6,7] make it difficult to control interface placement with the desired chemical composition profile for various types of actual device structures.

From the viewpoint of actual device processing, especially that necessary to achieve good ohmic and Schottky contacts to *p*-GaN, several efforts were devoted to characterizing and controlling the *p*-GaN surfaces in connection with pretreatment processes for metal deposition. Wu and Kahn[8,9] and Hartlieb *et al.*[10] prepared oxide- and contamination-free *p*-GaN surfaces by the N^+ sputtering process combined with high-temperature annealing and an ammonia-based high-temperature chemical vapor process, respectively. On those clean surfaces, however, they found the large band bending of more than 1.0 eV is probably due to the existence of surface states. Kim and co-workers[11] pointed out that an annealing process at 500 °C in ultrahigh vacuum (UHV) increased the band bending of 0.5 eV at the *p*-GaN surface compared with that on the HF-treated surface. These results indicate the difficulty in controlling *p*-GaN surfaces. Simple removal of oxide or contamination from the surface does not directly lead to improvement of the surface electronic properties of *p*-GaN. Nevertheless, chemical and electronic properties of Mg-doped *p*-GaN surfaces remain poorly understood.

This article presents a systematic investigation of the accumulation of Mg and its effects on the chemical and electronic properties of Mg-doped GaN surfaces by x-ray photoelectron spectroscopy (XPS) and Auger electron spectroscopy (AES).

II. EXPERIMENT

Mg-doped GaN samples grown on sapphire substrates by metalorganic vapor phase epitaxy (MOVPE) were used in this study. The samples were supplied by three different institutes in Japan. The sample structure consists of a low-temperature buffered layer/undoped layer/Mg-doped layer with thicknesses of 20 nm, 1.0 μm, and 2.0 μm, respectively. The doping concentration of Mg ranged from 3×10^{19} to $9\times10^{19}\,\mathrm{cm}^{-3}$ as measured by secondary ion mass spectroscopy (SIMS). An activation annealing process at 800 °C resulted in hole concentrations of $4\times10^{17}-7\times10^{17}\,\mathrm{cm}^{-3}$ at RT. The mobility ranged from 6 to $10\,\mathrm{cm}^2/\mathrm{V\,s}$. For comparison, a Si-doped *n*-GaN layer with a doping density of $2\times10^{17}\,\mathrm{cm}^{-3}$ grown by MOVPE on a sapphire substrate was also prepared.

Figure 1 shows typical Raman spectra of the *n*-GaN:Si and *p*-GaN:Mg samples obtained at RT by backscattering placement from the *c* face. Since we used an Ar^+ laser (514.5 nm) as an exciting source, the spectra obtained were not surface sensitive but bulk dominant. It should be noted that the difference in peak intensities from the sapphire substrates (sapphire E_g) is due to the difference in thickness

a)Electronic mail: hashi@rciqe.hokudai.ac.jp

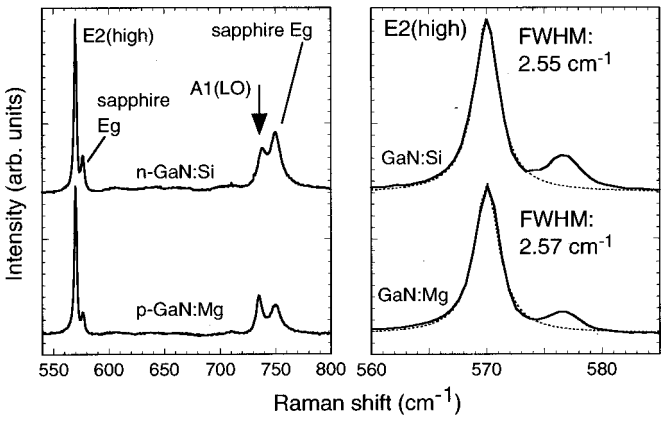

FIG. 1. Typical Raman spectra of the *n*-GaN:Si and *p*-GaN:Mg samples obtained at RT by backscattering from the *c* face.

of GaN layers between two samples. The wide scan data showed no pronounced difference in GaN Raman spectra. For both samples, the dominant *E*2 (high) vibration modes showed very similar spectra with the same linewidth, in good agreement with the calculated Lorentzian shapes indicated by the broken lines in Fig. 1(b). This indicated that the Mg-doped *p*-GaN layer has bulk quality comparable to that of the Si-doped GaN layer.

The sample surfaces were treated with KOH or NH_4OH solutions at 50 °C for 5 min. Some surfaces were then exposed to a remote N_2 plasma excited by an electron cyclotron resonance (ECR) source with a microwave (2.75 GHz) power of 50 W. The temperature and time of treatment were 300 °C and 1 min, respectively. Surface properties of the Mg-doped GaN layers were investigated by XPS and AES using a PHI 1600C system equipped with a spherical capacitor analyzer and a monochromated Al $K\alpha$ x-ray source ($h\nu = 1486.6$ eV). Energy calibration of the spectra was done carefully by separate measurement of Cu $2p_{3/2}$, Ag $3d_{5/2}$ and Au $4f_{7/2}$ peak positions using standard metal samples. The photovoltaic effect on the energy position of the XPS spectra measured was checked by varying the x-ray source power and by using external UV illumination from a Hg arc lamp. The results indicated that the shift of the peak due to this effect was within 0.1 eV.

III. RESULTS AND DISCUSSION

A. Air-exposed and chemically treated *p*-GaN surfaces

Figure 2 shows typical AES and XPS spectra obtained from the *p*-GaN sample with a Mg doping density of $9 \times 10^{19}\,\mathrm{cm}^{-3}$. For all the air-exposed and chemically treated samples, the Mg peaks were always detected together with Ga, N and O peaks in the AES spectra as well as in the XPS spectra even using very shallow escape angles of 10° or less. The apparent density of Mg calculated from the AES intensity and the XPS integrated intensity was $1.6 \times 10^{21}\,\mathrm{cm}^{-3}$. This is more than one order higher than the value in bulk determined by SIMS. For the calculation, separate XPS and AES measurements were made to calibrate the sensitivity

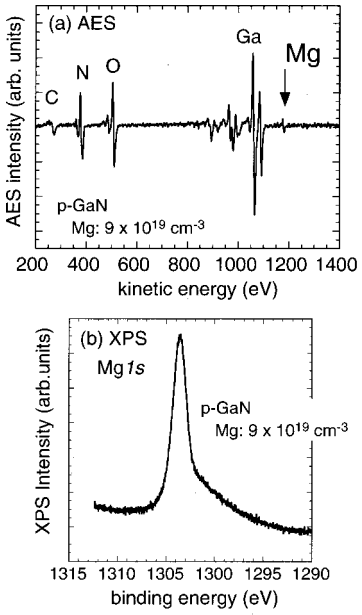

FIG. 2. Typical AES and XPS Mg 1*s* spectra obtained from the *p*-GaN sample with a Mg doping density of $9 \times 10^{19}\,\mathrm{cm}^{-3}$.

factors using the *n*-GaN sample (without Mg doping) and the crystalline Ga_2O_3 and MgO. Figure 3(a) shows a narrow scan XPS spectrum of the *p*-GaN sample with the lowest Mg-doping density, $3 \times 10^{19}\,\mathrm{cm}^{-3}$. For comparison, a spectrum of the *n*-GaN:Si surface was plotted in Fig. 3(b) that originated from the Ga 2*s* core level. By subtracting spectrum (b) from spectrum (a), minute Mg 1*s* peak was detected, as shown in Fig. 3(c). Even in this case, the calculated Mg density became $4 \times 10^{20}\,\mathrm{cm}^{-3}$, much higher than the actual doping density determined by SIMS. These results clearly indicate the accumulation or segregation of Mg on the Mg-doped GaN surface. Chang and co-workers[6] detected Mg accumulation by AES on the surface of GaN with bulk Mg density of $2-3 \times 10^{19}\,\mathrm{cm}^{-3}$ (determined by SIMS). Romano and co-workers[12] reported a SIMS profile in which the Mg

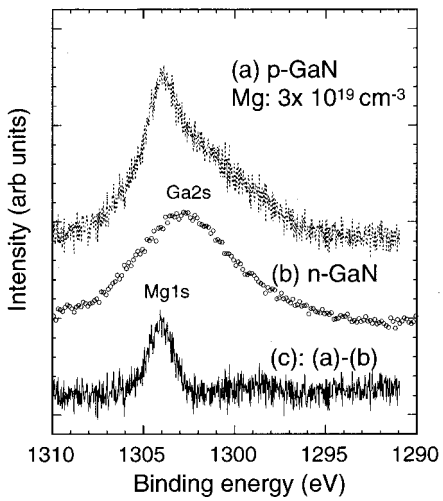

FIG. 3. XPS spectra from (a) the *p*-GaN sample with the lowest Mg density of $3 \times 10^{19}\,\mathrm{cm}^{-3}$ and (b) the *n*-GaN:Si sample. (c) Subtraction of (b) from (a).

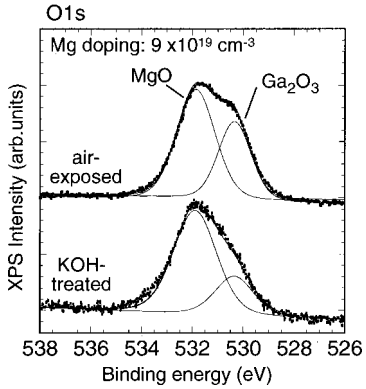

FIG. 4. The O 1*s* spectra of air-exposed and KOH-treated GaN:Mg surfaces.

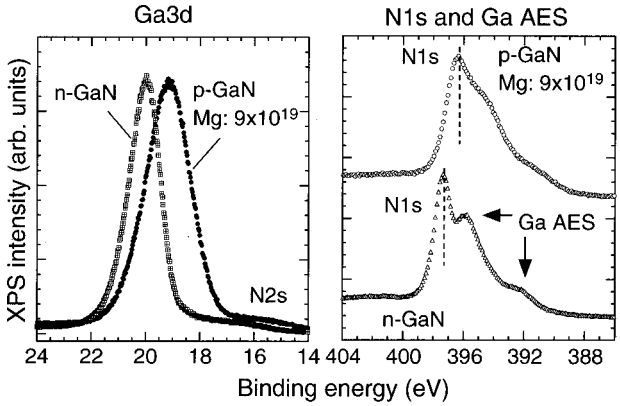

FIG. 5. Ga 3*d* and N 1*s* core-level spectra of the *p*-GaN:Mg surface after KOH treatment.

and oxygen concentrations increased near the surface region of Mg-doped GaN. Nakano and Jimbo[13] recently pointed out outdiffusion of Mg to the surface during activation annealing above 800 °C. These observations seem to support the possibility of accumulation or segregation of Mg on Mg-doped *p*-GaN surfaces.

Figure 4 shows observed O 1*s* spectra of air-exposed and the KOH-treated GaN:Mg surfaces. The air-exposed surface included two peaks that correspond to the Ga-oxide (Ga_2O_3) and Mg-oxide components. This implies that the excess Mg partly formed its oxide bond in the near-surface region of $p-$GaM:Mg. Only a slight decrease of the O 1*s* peak intensity was observed for the Ga-oxide phase after KOH treatment at 50 °C for 5 min, whereas the Mg-oxide phase remained unchanged after treatment. Similar spectra were obtained for the sample treated in the NH_4OH solution. Several groups[14–16] reported broad asymmetric O 1*s* spectra on air-exposed *p*-GaN:Mg surfaces and residue of O 1*s* traces even after various kinds of chemical wet treatment. Although no details of the analysis on Mg-related XPS spectra were described in that literature, there is a possibility that their O 1*s* spectra also included a Mg-oxide component. This feature is very different from the fact that Ga_2O_3 is the dominant natural oxide on the *n*-GaN:Si surface and it is essentially removed by chemical treatment in alkaline solutions.[17,18]

Ga 3*d* and N 1*s* core-level spectra of the *p*-GaN:Mg surface after KOH treatment are shown in Fig. 5. For comparison, the spectra of the reference MOVPE *n*-GaN layer are also plotted. The value of the full width at half maximum (FWHM) of the Ga 3*d* core level for the Mg-doped GaN surface was much larger than that of the reference MOVPE *n*-GaN, probably due to the presence of a large amount of Ga oxide, as shown in Fig. 4. A similar result was obtained in the N 1*s* spectra of the *p*-GaN sample where the separation between the N 1*s* and Ga AES peaks is indistinct. These results indicated that a surface disordered region including excess Mg and large amounts of oxides formed on the *p*-GaN:Mg surfaces, as schematically shown in Fig. 6. The KOH and NH_4OH treatments had little effect on the removal of such a disordered region. It was estimated from angle-resolved XPS analysis that the thickness of such a disordered region ranged from 3.0 to 4.0 nm. In addition, the difference in core-level peak energy between *p*-GaN and *n*-GaN samples was found to be 1.0 eV at most, as shown in Fig. 5. This value is very much lower than the 3.0 eV expected from the difference in Fermi energy between *p*- and *n*-GaN samples, and indicates pronounced upward and downward band bending of *n*-GaN and *p*-GaN surfaces, respectively.

To investigate surface electronic properties of *p*-GaN:Mg, valence band spectra were measured. The spectrum near the valence band maximum (VBM) edge is shown in Fig. 7(a) for the sample with a Mg density of $9\times19^{19}\,\mathrm{cm}^{-3}$. From linear extrapolation of the leading edge of the spectrum, the surface Fermi level (E_{FS}) was found to lie at $E_{VS}+1.4\,\mathrm{eV}$, as shown in Fig. 7(a), resulting in large downward band bending of 1.2–1.3 eV. The difference in energy between E_{VS} and the Ga 3*d* core-level peak was 17.8 eV, consistent with the value reported by Waldrap and Grant.[19] This large band bending implies that the surface disordered region including excess Mg and oxides introduced high-density surface states on the *p*-GaN surface, and led to strong Fermi level pinning at the surface. Bermudez,[20] Dhesi *et al.*,[21] and Wu and Kahn[9] have reported that a clean GaN (1×1) surface prepared by N^+ sputtering and high-temperature annealing (900 °C) showed a strong surface state contribution to ultraviolet photoemission spectroscopy (UPS) spectra at or near the VBM. Hartlieb *et al.*[10] also showed a similar UPS spectrum of the GaN surface annealed in NH_3 at 825–860 °C [chemical vapor clean (CVC) process]. They argued that such surface states are intrinsic, and

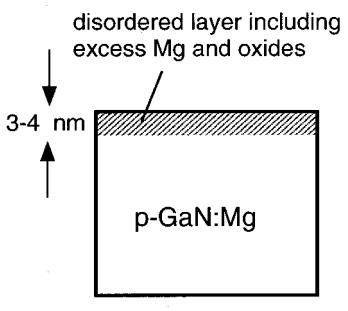

FIG. 6. Schematic of the air-exposed *p*-GaN:Mg surface.

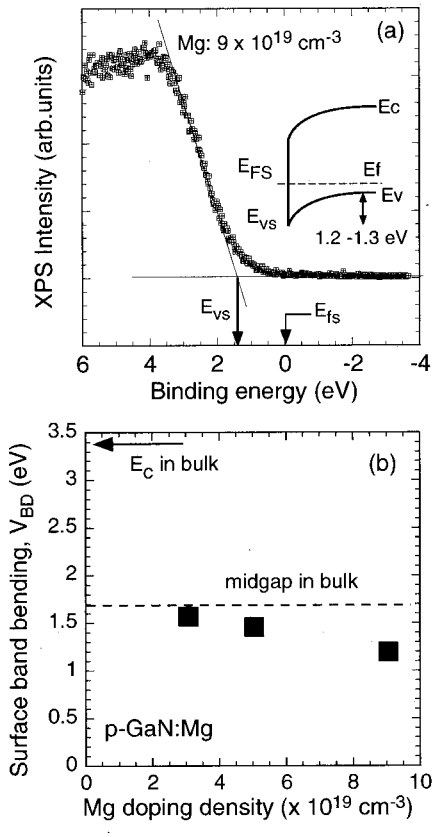

FIG. 7. (a) XPS spectrum near the valence band maximum edge of the sample with a Mg density of $9\times10^{19}\,\mathrm{cm}^{-3}$. (b) Surface band bending as a function of the Mg doping density.

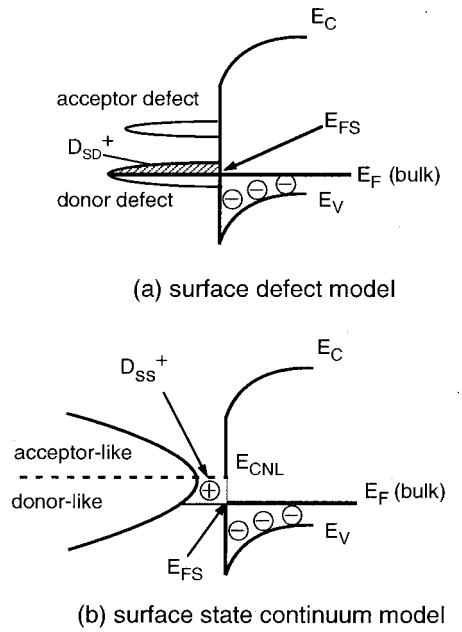

FIG. 8. Surface models for the firm Fermi level pinning.

probably originate from surface dangling bonds. However, no such surface state appeared in the XPS VB spectra shown in Fig. 7(a) (i.e., no shoulder near the VBM). One of the possible reasons for this is that the surface state effect is very weak in the XPS spectra compared to in the surface-sensitive UPS spectra. In fact, Wu and Kahn[9] showed the difference between the UPS and XPS VB spectra. Another possibility is that the surface electronic states of the air-exposed samples may be different from those of the clean GaN (1×1) surfaces reported by other groups. It is thought that the surface electronic states of semiconductors are very sensitive to contamination, adsorbants, order or disorder in chemical bonds, defects, etc. on the surfaces. For the air-exposed surface, the extrinsic surface states near midgap may be more dominant than the intrinsic states at or near the VBM.[10]

The change in band bending, V_{BD}, as a function of the Mg doping density is plotted in Fig. 7(b). The band bending was found to increase with a decrease in the Mg doping density. This behavior can be explained by a firm Fermi level pinning effect based on the surface defect model[22,23] or the surface state continuum model,[24] schematically shown in Figs. 8(a) and 8(b), respectively. When high-density surface defect levels and/or surface state continuum are introduced at the surface, the Fermi level position is fixed at E_{FS} which can balance surface charge from surface defects or states with space charge in the semiconductor depletion layer. Thus, pinning position E_{FS} is strongly related to the energy levels of the surface defects or the charge neutrality level, E_{CNL}, of the state continuum.[25] Mönch reported that E_{CNL} lies at $E_V+2.37\,\mathrm{eV}$ for GaN from calculation using the empirical tight-binding approximation.[26] If the surface has a discrete donor level according to the defect model[22] or the amphoteric defect model[23] shown in Fig. 8(a), the energy distribution of the level is expected to be equivalent to several kT (k is the Boltzmann constant and T is the absolute temperature), i.e., less than 0.1 eV at room temperature. Thus the change of 0.4 eV in band bending observed in Fig. 7(b) is indicative of the existence of a surface state continuum or its combination with defect levels that have a relatively wide distribution of energy on the *p*-GaN surface, as shown in Fig. 8(b). Using the values of V_{BD} obtained and $E_{\mathrm{CNL}}=E_V+2.37\,\mathrm{eV}$, simple estimation gave density of $7\times10^{12}-1\times10^{13}\,\mathrm{cm}^{-2}$ for the surface states near midgap.

B. Effects of ECR N_2-plasma treatment

Since the surface disorder region could be removed by neither the KOH nor NH_4OH wet chemical treatment, ECR-N_2 remote plasma treatment was employed to modify the chemical and electronic properties of *p*-GaN:Mg surfaces. Our previous study revealed that ECR-N_2 remote plasma treatment is very effective in realizing a well-ordered and nearly oxide-free surface of *n*-GaN with low surface state density.[17] N_2 remote plasma treatment at 300 °C for 1 min dramatically modified the surface chemistry of the Mg-doped GaN. Figure 9(a) shows O 1*s* XPS spectra of the sample with a Mg doping density of $9\times10^{19}\,\mathrm{cm}^{-3}$ before and after ECR-N_2 plasma treatment. A significant reduction of the O 1*s* XPS peak was observed after N_2 plasma treatment. The concentration of residual oxygen was estimated to be 1.1 at. % from the O 1*s* integrated intensity and the corresponding XPS sensitivity factor. Dhesi *et al.*,[21] Wu and

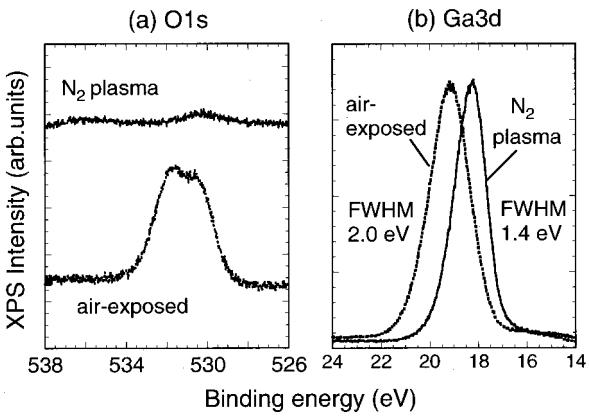

FIG. 9. O 1*s* and Ga 3*d* spectra of the sample with a Mg doping density of $9\times10^{19}\,\mathrm{cm}^{-3}$ before and after ECR-N_2 plasma treatment at 300 °C for 1 min.

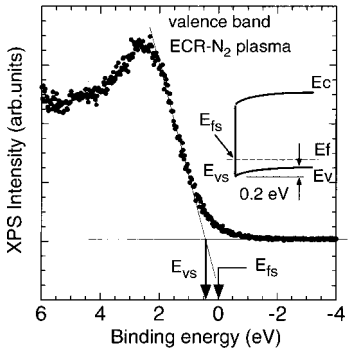

FIG. 10. Valence band spectrum of the *p*-GaN sample with a Mg doping density of $9\times10^{19}\,\mathrm{cm}^{-3}$ after ECR N_2 plasma treatment at 300 °C for 1 min.

Kahn,[9] and Hartlieb *et al.*[10] have reported similar concentrations of residual oxygen on GaN surfaces after the cleaning processes. In addition, the peak intensity of the Mg 1*s* level on the N_2-plasma treated surface was below the limit of detection. This surface process also brought pronounced changes in the XPS core-level spectra, as shown in Fig. 9(b). Sharpening of the linewidth and a remarkable peak shift toward lower binding energies were observed in the Ga 3*d* core-level spectrum after ECR-N_2 plasma treatment. The FWHM values obtained for the Ga 3*d* and N 1*s* core levels were comparable to those of the reference MOVPE *n*-GaN, indicating the recovery from the disorder of the chemical bonding configuration.

The mechanism of oxide removal during ECR-N_2 plasma treatment is not clear yet. It is unlikely that a physical sputtering effect is dominant for the dramatic changes in the surface chemistry of Mg-doped GaN. The present process utilized a remote ECR plasma that was separate from the ECR discharge region. In the ECR plasma stream, electrons and ions move with the same diffusion coefficient, i.e., so-called ambipolar diffusion.[27] This means that a near neutral condition can be maintained in the ECR plasma stream. In addition, ECR microwave discharge can be produced without large potential. Thus, it is expected that the self-biasing effect is rather weak in ECR plasma processes. In fact, Matsuoka and Ono[28] reported that the self-bias voltage was less than $-40\,\mathrm{V}$ in the gas pressure range of $1\times10^{-2}-1\times10^{-1}$ Pa. This as well as low ion energies of 10 to several tens of eV in the ECR plasma[28,29] can suppress an ion bombardment (sputtering) effect on the material surfaces. A possible surface process seems to start from the chemical reactions of reactive N radicals and ions on the Mg–O and Ga–O bonds in the surface disordered region. Then O atoms dissociated from MgO and Ga_2O_3 could react with each other or with N atoms and form volatile molecules such as O_2 and NO_x that can desorb from the surface along with Mg and Ga atoms as well as part of the oxide clusters. Ziemann and Castleman[30] suggested a similar evaporation or desorption process of MgO clusters based on their mass-spectroscopic study.

Figure 10 shows a valence band spectrum of a *p*-GaN sample with a Mg doping density of $9\times10^{19}\,\mathrm{cm}^{-3}$ after ECR-N_2 plasma treatment. The surface Fermi level, E_{FS}, was found to lie at $E_{VS}+0.4\,\mathrm{eV}$, corresponding to very weak band bending of 0.2 eV. This is consistent with the peak shift of 1.1 eV toward lower binding energies in the Ga 3*d* core level, shown in Fig. 9(b). Wu and Kahn[8,9] and Hartlieb *et al.*[10] reported large band bending of more than 1.0 eV even at oxide- and contamination-free *p*-GaN surfaces. This indicated that removal of an oxide layer from the surface is not directly connected with making the surface free of surface states. Again, the present process used ECR-excited N_2 plasma with low ion energies of 10 to several tens of eV. On the other hand, the energy for the N^+ sputtering (ion bombardment) process used by Wu and Kahn was 0.5 keV. Such an ion bombardment process at high temperature (900 °C) may induce some kind of defects near the surface region of GaN even though the process can remove contamination and natural oxides from the surface. In addition, the process temperatures used in the other approaches ranged from 825 to 900 °C,[8–10] much higher than the present process temperature of 300 °C. Several studies[31–33] indicated a temperature range of 800–900 °C as the threshold for surface deterioration of GaN, including the loss of N atoms. In addition, scanning tunneling microscopy (STM) images obtained by Packard and co-workers[34] of GaN surfaces prepared by annealing at 900 °C in UHV showed that these surfaces are highly defective and exhibit numerous arrangements of ordered N vacancies. Thus, there is a question of whether high-energy or high-temperature processes cause the degradation of electronic properties of GaN surfaces. On the other hand, the present low-energy low-temperature process utilizing remote ECR-N_2 plasma is quite suitable for suppressing the surface damage on GaN. In fact, the ECR-N_2 plasma process also achieved low interface state densities in the SiN_x/n-GaN system.[17,35] Theoretical calculation[36,37] predicted the lowest formation energy of N vacancies among native point defects in *p*-GaN. One of the possible reasons for achieving a nearly flat band condition on the *p*-GaN surface is that the present ECR-N_2 remote plasma treatment may partially recover or terminate N-vacancy related surface defects, and lead to a reduction of surface states.

IV. SUMMARY

The accumulation of Mg and its effects on the chemical and electronic properties of *p*-GaN surfaces were systematically investigated by AES and XPS. Pronounced accumulation of Mg was found on air-exposed and chemically treated *p*-GaN surfaces. The apparent density of Mg calculated from the XPS integrated intensity and the AES intensity was more than one order higher than the value of the bulk determined by SIMS. The Mg accumulation as well as large amounts of oxides formed in the disordered region on *p*-GaN:Mg surfaces. Large surface band bending of 1.2–1.6 eV was found at the surfaces even after KOH and NH_4OH treatment due to surface states with a density of $7\times10^{12}\,\mathrm{cm}^{-2}\,\mathrm{eV}^{-1}$ or higher. ECR-assisted N_2-plasma treatment at 300 °C for 1 min was effective in removing this surface disordered region and reducing surface band bending at the *p*-GaN:Mg surface.

ACKNOWLEDGMENTS

This work was partly supported by a grant-in-aid for Scientific Research (B) (Grant No. 14350155) from the Ministry of Education, Culture, Sports, Science and Technology and by a grant from the Support Center for Advanced Telecommunications Technology Research (SCAT).

[1] F. A. Reboredo and S. T. Pantelides, Phys. Rev. Lett. **82**, 1887 (1999).
[2] Z. Liliental-Weber, M. Benemara, W. Swider, J. Washbum, I. Grzegory, S. Porowski, D. J. H. Lambert, C. J. Eiting, and R. D. Dupuis, Appl. Phys. Lett. **75**, 4159 (1999).
[3] P. Vennegues, M. Benaissa, B. Beaumont, E. Feltin, P. D. Mierry, S. Dalmasso, M. Leroux, and P. Gibart, Appl. Phys. Lett. **77**, 880 (2000).
[4] G. Martinez-Criado, A. Cros, A. Cantarero, R. Dimitrov, O. Ambacher, and M. Stutzmann, J. Appl. Phys. **88**, 3470 (2000).
[5] Z. Liliental-Weber, J. Jasinski, M. Benemara, I. Grzegory, S. Porowski, D. J. H. Lambert, C. J. Eiting, and R. D. Dupuis, Phys. Status Solidi B **228**, 345 (2001).
[6] T. S. Chang, S. V. Novikov, C. T. Foxon, and J. W. Orton, Solid State Commun. **109**, 439 (1999).
[7] A. J. Ptak, T. H. Myers, L. T. Romano, C. G. Van de Walle, and J. E. Northrup, Appl. Phys. Lett. **78**, 285 (2001).
[8] C. I. Wu and A. Kahn, J. Vac. Sci. Technol. B **16**, 2218 (1998).
[9] C. I. Wu and A. Kahn, J. Appl. Phys. **86**, 3209 (1999).
[10] P. J. Hartlieb, A. Roskowski, R. F. Davis, A. Platow, and R. J. Nemanich, J. Appl. Phys. **91**, 732 (2002).
[11] M.-H. Kim, S.-N. Lee, C. Huh, S. Y. Park, J. Y. Han, J. M. Seo, and S.-J. Park, Phys. Rev. B **61**, 10966 (2000).
[12] L. T. Romano, M. Kneissl, J. E. Northrup, C. G. Van de Walle, and D. W. Treat, Appl. Phys. Lett. **79**, 2734 (2001).
[13] Y. Nakano and T. Jinbo, J. Appl. Phys. **92**, 5590 (2002).
[14] J.-L. Lee and J. K. Kim, J. Electrochem. Soc. **147**, 2297 (2000).
[15] I. Waki, H. Fujioka, K. Ono, M. Oshima, H. Miki, and A. Fukizawa, Jpn. J. Appl. Phys., Part 1 **39**, 4451 (2000).
[16] Y.-J. Lin, C.-D. Tsai, Y.-T. Lyu, and C.-T. Lee, Appl. Phys. Lett. **77**, 687 (2000).
[17] T. Hashizume, S. Ootomo, S. Oyama, M. Konishi, and H. Hasegawa, J. Vac. Sci. Technol. B **19**, 1675 (2001).
[18] T. Hashizume, R. Nakasaki, S. Ootomo, S. Oyama, and H. Hasegawa, Mater. Sci. Eng., B **80**, 309 (2001).
[19] J. R. Waldrop and R. W. Grant, Appl. Phys. Lett. **68**, 2879 (1996).
[20] V. M. Bermudez, J. Appl. Phys. **80**, 1190 (1996).
[21] S. S. Dhesi, C. B. Stagarescu, K. E. Smith, D. Doppalapudi, R. Singh, and D. Moustakas, Phys. Rev. B **56**, 10271 (1997).
[22] W. E. Spicer, Z. Liliental-Weber, E. Weber, N. Newman, T. Kedelewicz, R. Cao, C. McCants, P. Mahowald, K. Miyano, and I. Lindau, J. Vac. Sci. Technol. B **6**, 1245 (1988).
[23] W. Walukiewicz, J. Vac. Sci. Technol. B **6**, 1257 (1988).
[24] H. Hasegawa and H. Ohno, J. Vac. Sci. Technol. B **4**, 1130 (1986).
[25] J. Tersoff, Phys. Rev. B **32**, 6968 (1985).
[26] W. Mönch, Appl. Surf. Sci. **117/118**, 380 (1997).
[27] J. Asmussen, J. Vac. Sci. Technol. A **7**, 883 (1989).
[28] M. Matsuoka and K. Ono, J. Vac. Sci. Technol. A **6**, 25 (1988).
[29] G. W. Gibson, Jr., H. H. Sawin, I. Tepermeister, D. E. Ibbotson, and J. T. C. Lee, J. Vac. Sci. Technol. B **12**, 2333 (1994).
[30] P. J. Ziemann and A. W. Castleman, Jr., Phys. Rev. B **44**, 6488 (1991).
[31] M. M. Sung, J. Ahn, V. Bykov, J. W. Rabalais, D. D. Koleske, and A. E. Wickenden, Phys. Rev. B **54**, 14652 (1996).
[32] O. Ambacher, H. Angerer, R. Dimitrov, W. Rieger, M. Stutzmann, G. Dollinger, and A. Bergmaier, Phys. Status Solidi A **159**, 105 (1997).
[33] M. A. Rana, H. W. Choi, M. B. H. Breese, T. Osipowicz, S. J. Chua, and F. Watt, Mater. Res. Soc. Symp. Proc. **743**, L 11.28.1 (2003).
[34] W. E. Packard, J. D. Dow, K. Doverspike, R. Kaplan, and R. Nicolaides, J. Mater. Res. **12**, 646 (1997).
[35] T. Hashizume and R. Nakasaki, Appl. Phys. Lett. **80**, 4564 (2002).
[36] J. Neugebauer and C. G. Van de Walle, Phys. Rev. B **50**, 8086 (1994).
[37] C. G. Van de Walle, C. Stampfl, and J. Neugebauer, J. Cryst. Growth **189/190**, 505 (1998).